



Förster resonance energy transfer competitive displacement assay for human soluble epoxide hydrolase

Kin Sing Stephen Lee^a, Christophe Morisseau^a, Jun Yang^a, Peng Wang^{a,b}, Sung Hee Hwang^a, Bruce D. Hammock^{a,*}

^a Department of Entomology and UCD Comprehensive Cancer Center, University of California, Davis, CA 95616, USA

^b Department of Applied Chemistry, China Agricultural University, Beijing 100193, People's Republic of China

ARTICLE INFO

Article history:

Available online 5 December 2012

Keywords:

Soluble epoxide hydrolase
Binding assay
Competitive displacement assay
Förster resonance energy transfer (FRET)
Fluorescent assay

ABSTRACT

The soluble epoxide hydrolase (sEH), responsible for the hydrolysis of various fatty acid epoxides to their corresponding 1,2-diols, is becoming an attractive pharmaceutical target. These fatty acid epoxides, particularly epoxyeicosatrienoic acids (EETs), play an important role in human homeostatic and inflammation processes. Therefore, inhibition of human sEH, which stabilizes EETs *in vivo*, brings several beneficial effects to human health. Although there are several catalytic assays available to determine the potency of sEH inhibitors, measuring the *in vitro* inhibition constant (K_i) for these inhibitors using catalytic assay is laborious. In addition, k_{off} , which has been recently suggested to correlate better with the *in vivo* potency of inhibitors, has never been measured for sEH inhibitors. To better measure the potency of sEH inhibitors, a reporting ligand, 1-(adamantan-1-yl)-3-(1-(2-(7-hydroxy-2-oxo-2H-chromen-4-yl)acetyl) piperidin-4-yl)urea (ACPU), was designed and synthesized. With ACPU, we have developed a Förster resonance energy transfer (FRET)-based competitive displacement assay using intrinsic tryptophan fluorescence from sEH. In addition, the resulting assay allows us to measure the K_i values of very potent compounds to the picomolar level and to obtain relative k_{off} values of the inhibitors. This assay provides additional data to evaluate the potency of sEH inhibitors.

© 2012 Elsevier Inc. All rights reserved.

In mammals, the soluble epoxide hydrolase (sEH)¹ (EC 3.3.2.10) metabolizes important signaling epoxy fatty acids to the corresponding 1,2-diols [1]. These epoxy fatty acids, particularly epoxyeicosatrienoic acids (EETs) from arachidonic acid and epoxides from omega-3 fatty acids, have been demonstrated to maintain blood pressure in several animal models, to resolve inflammatory disorders and reduce pain, and generally to maintain homeostasis [2–9]. Therefore, stabilization of EETs through inhibition of sEH could be beneficial to human health. Over the past decade, significant progress has been made toward the clinical development of sEH inhibitors [10].

Catalytic assays for sEH have been instrumental in obtaining improved sEH inhibitors. Over the years, numerous substrate-

based assays have been developed and used [11–20]. Existing sEH assays are able to distinguish among inhibitors of varying potency down to low nanomolar. However, as the inhibitor concentration approaches the enzyme concentration, the assays cannot distinguish among the most potent inhibitors. Several laboratories have reached this sensitivity limit with compounds they have made [5,10,21], so an assay capable of distinguishing among highly potent inhibitors would be attractive.

Catalytic assays for enzymes and their inhibitors are attractive for many mechanistic reasons; however, binding assays lend themselves to high-throughput formats easier than enzymatic assays. In general, the different sEH catalytic assays rank compounds in similar order, but there are notable exceptions. A binding assay with the enzyme in which catalysis plays no role could simplify data interpretation. Several binding assays have been described for sEH [13,16]. In 2009, Eldrup and coworkers reported the use of a tetramethyl rhodamine-labeled probe to measure human or rat sEH inhibition [13]. However, such an assay requires spectrometers that can measure fluorescence polarization in order to distinguish the bound probe from background. In a similar approach, urea-based inhibitors containing aryl groups are able to quench sEH intrinsic tryptophan fluorescence. However, to observe fluorescent quenching through binding to inhibitors, a relatively high

* Corresponding author. Fax: +1 530 752 1537.

E-mail address: bdhammock@ucdavis.edu (B.D. Hammock).

¹ Abbreviations used: sEH, soluble epoxide hydrolase; EET, epoxyeicosatrienoic acid; IC₅₀, half-maximal inhibitory concentration; FRET, Förster resonance energy transfer; 14,15-EET, 14,15-epoxyeicosatrienoic acid; PTU, 1-(piperidine-4-yl)-3-(4-(trifluoromethyl)phenyl)urea; DMSO, dimethyl sulfoxide; ACPU, 1-(adamantan-1-yl)-3-(1-(2-(7-hydroxy-2-oxo-2H-chromen-4-yl)acetyl)piperidin-4-yl)urea; EDCl, 1-ethyl-3-(3-dimethylaminopropyl)carbodiimide; DMAP, 4-dimethylaminopyridine; rt, room temperature; DMF, dimethylformamide; hsEH, human sEH; LC-MS/MS, liquid chromatography-tandem mass spectrometry; PB buffer, sodium phosphate buffer; *t*-DPPPO, *trans*-diphenyl-propene oxide; CMNPC, cyano(6-methoxy-naphthalen-2-yl)methyl *trans*-[(3-phenyloxy)ran-2-yl)methyl] carbonate; msEH, mouse sEH.

concentration of enzyme is needed (50–100 nM), making this assay costly. In addition, several recent inhibitors developed by several groups have nanomolar or sub-picomolar half-maximal inhibitory concentration (IC₅₀) values. Because the binding probes used in the above assay do not bind the sEH tightly (IC₅₀ ~1 μM), it is not suitable to measure the binding of very potent inhibitors with K_i values lower than 10 nM [16].

With some inhibitors, such as cyclooxygenase inhibitors, residency time on the enzyme correlates better with in vivo efficacy than does enzyme inhibition potency [22]. Thus, an assay that could estimate occupancy time of the sEH inhibitors will be an invaluable tool to provide another dimension to estimate the in vivo potency of these inhibitors. However, none of the described assays is able to measure the *k*_{off} of the inhibitor directly [13]. Here, we report a newly developed Förster resonance energy transfer (FRET)-based displacement assay using fluorescence from intrinsic tryptophan to measure the binding affinity (K_i) and relative *k*_{off} of very potent inhibitors of sEH.

Materials and methods

Chemicals

All reagents and solvents were purchased from Fisher Scientific, Acros Organics, TCI America Fine Chemicals, and Sigma-Aldrich and were used directly without further purification. 14,15-Epoxyecosatrienoic acid (14,15-EET) was purchased from Cayman Chemicals. The syntheses of *tert*-butyl 4-(3-(adamantan-1-yl)ureido)piperidine-1-carboxylate, *tert*-butyl 4-(3-(4-(trifluoromethyl)phenyl)ureido)piperidine-1-carboxylate, 1-(adamantan-1-yl)-3-(piperidin-4-yl)urea, 1-(piperidin-4-yl)-3-(4-(trifluoromethyl)phenyl)urea (PTU), and 1-((1*r*,4*r*)-4-hydroxycyclohexyl)-3-(4-(trifluoromethoxy)phenyl)urea have been reported elsewhere [5,21,23,24]. All reactions for this study were carried out in a dry nitrogen atmosphere unless otherwise specified. Reactions were monitored by thin-layer chromatography on Merck F₂₅₄ silica gel 60 aluminum sheets, and spots were either visible under light or ultraviolet light (254 nm) or stained with an oxidizing solution (KMnO₄ stain). Column chromatography was performed with silica gel.

¹H NMR spectra were recorded on a Varian QE-300 spectrometer with deuterated chloroform (CDCl₃, δ = 7.24 ppm) or deuterated dimethyl sulfoxide (DMSO-*d*₆) containing TMS as an internal standard. ¹³C NMR spectra were recorded on a Varian QE-300 spectrometer at 75 MHz. ¹⁹F NMR spectra were recorded on a Varian QE-300 spectrometer at 282.4 MHz.

Synthesis of 1-(adamantan-1-yl)-3-(1-(2-(7-hydroxy-2-oxo-2H-chromen-4-yl)acetyl)piperidin-4-yl)urea (ACPU)

1-(Adamantan-1-yl)-3-(piperidin-4-yl)urea (50 mg, 180 μmol) [23], 1-ethyl-3-(3-dimethylaminopropyl)carbodiimide (EDCI, 34.4 mg, 180 μmol), 4-dimethylaminopyridine (DMAP, 21.8 mg, 180 μmol), and 7-hydroxycoumarin-4-acetic acid (39.6 mg, 180 μmol) were dissolved in CH₂Cl₂ (50 ml). The reaction vessel was wrapped with aluminum foil, and the reaction mixture was stirred for 12 h at room temperature (rt). The reaction was quenched by the addition of aqueous HCl solution (0.1 M), and the organic layer was collected. The aqueous layer was extracted by CH₂Cl₂ five times, and the combined organic layers were dried over anhydrous MgSO₄. The crude product was concentrated and further purified by flash chromatography. The final product was eluted with 2% MeOH in EtOAc, resulting in pale yellow solid (56 mg, 116 μmol, 65% yield). ¹H NMR (300 MHz, DMSO-*d*₆) δ 10.57 (br, 1H), 7.48 (d, *J* = 9 Hz, 1H), 6.77 (dd, *J* = 9 and 1 Hz, 1H), 6.71 (d, *J* = 1 Hz), 6.08 (s, 1H), 5.71 (d, *J* = 7.5 Hz, 1H), 5.42 (s, 1H), 4.08

(d, *J* = 14 Hz, 1H), 3.94 (s, 2H), 3.82 (d, *J* = 14 Hz, 1H), 3.55 (m, 1H), 3.20 (t, *J* = 11 Hz, 1H), 2.84 (t, *J* = 11 Hz, 1H), 1.99 (s, 3H), 1.85 (s, 6H), 1.76 (m, 2H), 1.59 (s, 6H), 1.11–1.30 (m, 2H).

Synthesis of 1-(1-(2-methylbutyryl)piperidin-4-yl)-3-(4-(trifluoromethyl)phenyl)urea (11)

2-Methylbutyric acid (50 mg, 0.487 mmol), DMAP (54.5 mg, 0.487 mmol), and EDCI (64 mg, 0.325 mmol) were dissolved in dimethylformamide (DMF, 10 ml). PTU (55 mg, 0.325 mmol) was dissolved in DMF (5 ml) and was added into the reaction mixture dropwise. The reaction mixture was stirred for 12 h at rt and was quenched by the addition of HCl solution (1 M, aq). The organic layer was collected, and the aqueous layer was extracted with EtOAc four times. The combined organic layer was concentrated in vacuo and further purified by flash chromatography (EtOAc/Hex, 2:1), yielding the final product (80 mg, 0.215 mmol, 66% yield). ¹H NMR (DMSO-*d*₆, 300 MHz): 8.77 (d, *J* = 8.4 Hz, 1H), 7.57 (s, 4H), 6.37 (s, 1H), 4.22 (m, 1H), 3.88 (d, *J* = 13.2 Hz, 1H), 3.71 (m, 1H), 3.17 (t, *J* = 12.8 Hz, 1H), 2.84 (m, 2H), 1.85 (m, 2H), 1.54 (m, 1H), 1.29 (m, 3H), 0.97 (s, 3H), 0.81 (d, *J* = 6 Hz, 3H).

Synthesis of 1-(1-(methanesulfonyl)piperidin-4-yl)-3-(4-(trifluoromethyl)phenyl)urea (12)

PTU (70 mg, 0.244 mmol) and Et₃N (30 mg, 0.292 mmol) were dissolved in DMF (10 ml) at 0 °C, and methylsulfonyl chloride (56 mg, 0.487 mmol) was added into the reaction mixture dropwise. The reaction mixture was stirred for 12 h at rt and was quenched by the addition of HCl solution (1 M). The organic layers were collected, and the aqueous layer was extracted with EtOAc four times. The combined organic layers were concentrated in vacuo and further purified by flash column chromatography (EtOAc/Hex, 6:4), yielding the final product (45 mg, 0.123 mmol, 51% yield). ¹H NMR (DMSO-*d*₆, 300 MHz): δ 8.82 (s, 1H), 7.57 (s, 4H), 6.39 (d, *J* = 7.5 Hz, 1H), 3.61 (m, 1H), 3.46 (d, *J* = 12.3 Hz, 2H), 2.87 (s, 3H), 2.87 (m, 2H), 1.92 (d, *J* = 9.9 Hz, 2H), 1.46 (m, 2H).

Synthesis of 1-(1-(butane-1-sulfonyl)piperidin-4-yl)-3-(4-(trifluoromethyl)phenyl)urea (13)

Butylsulfonyl chloride (76 mg, 0.487 mmol) was reacted with PTU (70 mg, 0.244 mmol) in the same manner as the synthesis of 1-(1-(methylsulfonyl)piperidin-4-yl)-3-(4-(trifluoromethyl)phenyl)urea, yielding the final product (65 mg, 0.160 mmol, 66% yield). ¹H NMR (*d*₆-DMSO, 300 MHz): δ 8.78 (s, 1H), 7.57 (s, 4H), 6.38 (d, *J* = 8 Hz, 1H), 3.82 (d, *J* = Hz, 1H), 3.62 (m, 1H), 3.50 (d, *J* = 12 Hz, 2H), 3.00 (m, 4H), 1.89 (d, *J* = 11 Hz, 2H), 1.66 (m, 2H), 1.40 (m, 4H), 0.90 (t, *J* = 8 Hz, 3H).

Enzyme preparation

Expression and purification of recombinant sEH followed the published procedure [25]. Briefly, the full-length human complementary DNA (cDNA) for sEH was expressed in high yield in a baculovirus system. The sEH activity in supernatant from cell culture was purified by affinity chromatography to yield high specific activity and apparent homogeneity on sodium dodecyl sulfate-polyacrylamide gel electrophoresis (see Fig. S1 in Supplementary material). The enzyme was frozen in multiple small aliquots and thawed once immediately before use.

IC₅₀ determination for hSEH inhibitors

IC₅₀ values of human sEH (hSEH) inhibitors were determined by three different assays (radiometric, fluorescent, and liquid chroma-

tography–tandem mass spectrometry [LC–MS/MS]) according to published procedures [14–18]. The assays are described in detail in the Supplementary material. IC₅₀ values were determined based on regression of at least five data points with a minimum of two points in the linear region of the curve on either side of the IC₅₀.

Fluorescence binding assay procedure

The fluorescent binding assay was carried out based on the published procedure with some modifications as described below [15]. All inhibitors were stored in glass containers to prevent them from being absorbed by plastic. Some plastic containers were found to leach fluorescent impurities into sample, which affects the fluorescence analysis. sEH was diluted in filtered sodium phosphate buffer (PB buffer, 100 mM, pH 7.4) with 0.01% gelatin (Sigma–Aldrich) to prevent the loss of sEH due to nonspecific binding to the surface of the cuvette. sEH (10 nM, 3 ml in phosphate buffer with 0.01% gelatin, pH 7.4) was added into the cuvette and was stirred gently. The solution was equilibrated at 30 °C for 5 min. The sample was excited at 280 nm, which is the λ_{\max} of the protein (see Fig. S3c in Supplementary material) (excitation slit width = 1.0 nm), and the emission at the protein peak maximum (325–360 nm, emission slit width = 12 nm) (Fig. S3a) and the emission of coumarin (450 nm, emission slit width = 12 nm) (Fig. S3b) were measured. Reporting ligand dissolved in EtOH was added to the sample at varying concentrations (0.2–20 nM). The total concentration of EtOH was kept under 2%. Measurement of emission was taken 60 min after each reporting ligand addition. The concentration of the reporting ligand was plotted against the relative fluorescence intensity. The titration was completed when there was no observable fluorescence quenching occurring in the 325- to 360-nm region and no linear increase of fluorescence at 450 nm on the addition of reporting ligand.

Because coumarin fluoresces on excitation at 283 nm and absorbs at 330 nm, which could quench the tryptophan fluorescence from the protein, a correction was made prior to calculating the binding constant for sEH with the reporting ligand. A blank titration of reporting ligand with 110 nM *N*-acetyltryptophan was performed, and the quenched fluorescence (at 320–360 nm) and enhanced fluorescence (at 450 nm) were added back to (for fluorescence from 320 to 360 nm) or subtracted from (for fluorescence at 450 nm) the actual titration data with sEH.

Curve fitting

The curve fitting was carried out with KaleidaGraph based on the published procedures [26,27]. The correction of fluorescence titration required four calculations on completion of both protein and blank titration with the reporting ligand (ACPU):

- (1) Determine α for each point of the titration:

$$\alpha = \frac{F_{\max} - F}{F_{\max} - F_0} \quad (1)$$

where α is fraction of free binding sites, F_{\max} is fluorescence on saturation, F is observed fluorescence, and F_0 is initial fluorescence.

- (2) Determine the free ligand concentration:

$$R = R_0 - nP_0(1 - \alpha) \quad (2)$$

where R_0 is ligand concentration, n is number of binding sites, and P_0 is protein concentration.

- (3) Estimate the fluorescence contribution of the free ligand, F_R , to be deduced from the blank (*N*-acetyltryptophanamide) titration.

- (4) Subtract the fluorescence contribution of the free ligand based on the actual readings and plot the corrected fluorescence values versus the ligand concentration: $(F - F_R)$ versus R_0 .

The K_d value for each sEH inhibitor was determined according to the method previously described by Wang and coworkers using the fluorescence values calculated above [28].

The dissociation constant is calculated by KaleidaGraph using nonlinear least squares regression analysis. The corrected relative fluorescence intensity is plotted against the concentration of each sEH inhibitor. The protein concentration and the final fluorescence intensity at saturation are determined in order for the program to calculate the dissociation constant:

$$\frac{F}{F_f} = 1 + \left(\frac{F_b}{F_f}\right) \times \left(\frac{P_t + R_t + K_d - \sqrt{(P_t + R_t + K_d)^2 - 4P_tR_t}}{2P_t}\right) \quad (3)$$

where F is observed fluorescence, F_f is fluorescence of free protein, F_b is fluorescence of bound protein, P_t is total protein concentration, and R_t is total reporting ligand concentration.

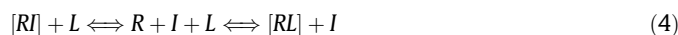
FRET displacement assay procedure

As mentioned, to prevent leaching of fluorescence impurities from the plastic tube and nonspecific binding to sEH inhibitors, the inhibitor was stored in glass vials. In addition, sEH was dissolved in phosphate buffer (100 mM sodium phosphate, pH 7.4, 0.01% gelatin) to avoid loss of protein from nonspecific binding to the cuvette surface. sEH (10 nM, 3 ml, 100 mM phosphate, pH 7.4, 0.01% gelatin) was stirred and preincubated with reporting ligand (1 equivalent) at 30 °C for 1 h in a quartz cuvette. The fluorescence (455 nm, emission slit width = 12 nm, excited at 280 nm, excitation slit width = 1.0 nm) was measured. The enzyme–ligand complex was titrated with different sEH inhibitors at varying concentrations until no more fluorescence quenching was observed. The relative fluorescence intensity was plotted against the concentration of inhibitor.

Curve fitting

The data manipulation and K_i calculation were based on the original article by Wang with some modifications suggested in the article by Roehrl and coworkers [29,30].

The displacement assay has three components, two ligands and one protein, which creates three-state equilibrium binding models:



The three-state equilibrium Eq. (4) is composed of the sEH–inhibitor complex, sEH, and the sEH–reporting ligand complex. The relative fluorescence intensity (F_3) was plotted against the concentration of sEH inhibitor, and the curve was fitted into Eq. (5) derived by Wang for three-state equilibrium [29]:

$$F_3 = [2(a^2 - 3b)^{1/2} \cos(\theta/3) - a] / \{3K_{d1} + [2(a^2 - 3b)^{1/2} \times \cos(\theta/3) - a]\} \quad (5)$$

with $a = K_{d1} + K_{d2} + L + I - R$;

$$b = K_{d2}(L - R) + K_{d1}(I - R) + K_{d1}K_{d2};$$

$$c = -K_{d1}K_{d2}R; \text{ and}$$

$$\theta = \arccos\{(-2a^3 + 9ab - 27c) / [2(a^2 - 3b)^{3/2}]\}.$$

where F_3 is relative fluorescence and is equal to (observed fluorescence – fluorescence at saturation)/(initiated fluorescence – fluores-

cence at saturation), I is concentration of added unlabeled competing ligand, R is total concentration of sEH, L is total concentration of reporting ligand, K_{d1} is dissociation constant of reporting ligand (found by fluorescent binding assay), and K_{d2} is inhibition constant of inhibitors.

k_{off} measurement procedure

sEH (8 μ M) was incubated with inhibitor (8.8 μ M, 100 mM PB buffer, pH 7.4) for 1.5 h at 30 °C. The sEH–inhibitor complex was diluted 40 times against 100 equivalents of ACPU (20 μ M, 100 mM PB buffer, pH 7.4). The fluorescence at 450 nm (excited at 280 nm) was measured every 30 s for 5000 s. The fluorescence (emission at 450 nm) was plotted against time (s). The resulting curve was fitted to single exponential growth, and the relative k_{off} was obtained. This procedure was then applied to other inhibitors using the same procedure as described above for ACPU.

Results and discussion

Design and synthesis of fluorescent reporter

hsEH is a predominantly cytoplasmic enzyme containing both epoxide hydrolase domain at the C terminus and phosphatase domain at the N terminus [31–33]. From the holo structure of hsEH with its inhibitor, *N*-cyclohexyl-*N'*-(4-iodophenyl)urea, 10 tryptophans are found on the C terminus near the catalytic cavity where the inhibitors bind (see Fig. S2 in Supplementary material) [32]. Such tryptophans, which absorb at 280 nm and fluoresce between 330 and 380 nm, are well-known intrinsic fluorophores that have been used routinely in biomedical and biochemical research to study protein–ligand or protein–protein interactions [26,27,34,35]. To develop a FRET displacement assay, we chose these intrinsic tryptophans as fluorescent donors, and a reporting ligand that contains the complementary fluorescent acceptors will be designed and synthesized.

Crystal structures showed that 3 tryptophans are located within the binding pocket. To position the fluorescent acceptor close to these tryptophans for maximizing FRET, a small fluorophore that can fit within the binding pocket is needed. In addition, a fluorophore whose absorption spectrum overlapped with the fluorescence of tryptophan is needed to enhance the energy transfer process. Besides, a fluorophore that has relatively high quantum yield can enhance FRET signal. Therefore, 7-hydroxycoumarin, which absorbs at 360 nm with a quantum yield around 0.6 [36], was chosen as the fluorescent acceptor for the reporting ligand (Fig. S3a). In addition, a relatively tight binding inhibitor scaffold is desired for the reporting ligand. From the large number of published structures of potent inhibitors [10], adamantane was selected as a functional group yielding highly potent inhibitors [5,21] and fitting tightly in the “small” binding pocket of the sEH enzyme while lacking an aromatic moiety that could quench the intrinsic tryptophan fluorescence of the sEH with a 300-nm broad absorbance band. For the “large” or right binding pocket on the 3 position of the urea, we selected a piperidyl group for the same reasons to give a 1-adamantyl-3-piperidyl scaffold. We wanted a reporting ligand with a low K_d to improve our ability to distinguish among inhibitors with K_i values in the nanomolar to picomolar (nM to pM) binding range [37]. Thus, our reporting ligand (ACPU), which contains one of the common hsEH inhibitor scaffolds, 1-adamantyl-3-piperidyl urea (A), and a fluorophore, coumarin (B), was designed and synthesized (Fig. 1A). Modeling of sEH with the reporting ligand suggests that ACPU should fit nicely inside the binding pocket, and 6 tryptophans are located within 12 Å of the coumarin (Fig. 1B).

Measuring binding constant (K_d) for fluorescent reporter (ACPU)

To determine a near optimal incubation time for each titration, the rate of binding between ACPU and hsEH was studied based on the FRET signal at 450 nm. The results indicated that 40 min was needed to reach the equilibrium between ACPU and sEH under the conditions described (Fig. S4). Then, hsEH was titrated with the ACPU to obtain the K_d of the reporting ligand. From the titration, we observed that the fluorescence at 348 nm from the protein decreased, whereas the fluorescence at 450 nm increased proportionally to the ACPU concentration, as would be expected from FRET (Fig. S5). Because the ACPU can also be excited at 280 nm, the fluorescence enhancement from the assay at 450 nm was corrected for background fluorescence at different concentrations before it was used to calculate the dissociation constant (K_d) of ACPU (see Materials and methods). Using the nonlinear regression analysis of the quadratic equation Eq. (3) derived from the thermodynamic and mass law [38], the K_d of ACPU for hsEH is calculated to be 1.04 ± 0.04 nM, indicating a tight binding ligand. This value is the same whether it is based on the fluorescence decrease at 340 nm or the fluorescence enhancement at 450 nm plotted against different concentrations of ACPU (Fig. 2). Compared with previous reporting ligands ($K_d = 1$ μ M) [13,16], the high potency of ACPU permits one to measure the K_i of very tight binding inhibitors accurately [37,39].

Development and optimization of competitive displacement assay with APCU

A competitive displacement assay based on the above-established FRET system was then developed to determine inhibition constants (K_i) for sEH inhibitors. Because the K_d of the ACPU is known, the K_i of the inhibitor can be calculated through measuring

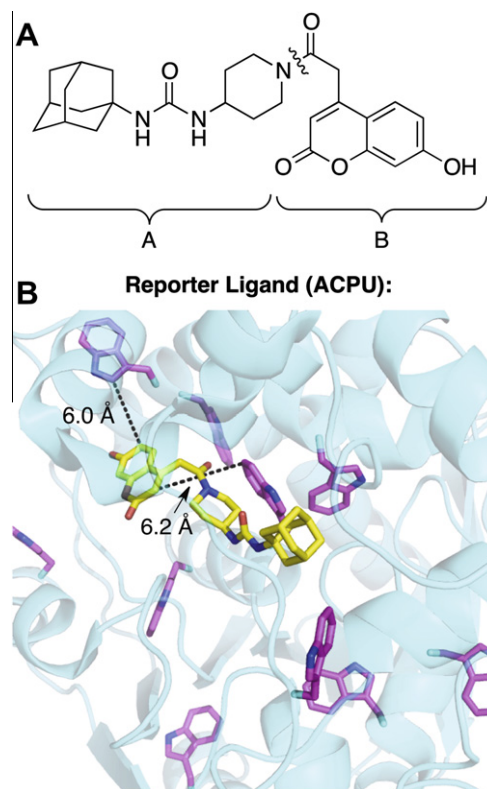


Fig. 1. (A) Structure of the reporting ligand (ACPU). (B) Model of ACPU within epoxide hydrolase binding site of hsEH based on the holo-hsEH crystal structure (PDB: 1VJ5) [32] with tryptophan labeled as color purple and ACPU colored as yellow. Two tryptophans within 6.5 Å of the coumarin of the bound reporting ligand are indicated, and their distances are shown next to the dotted line.

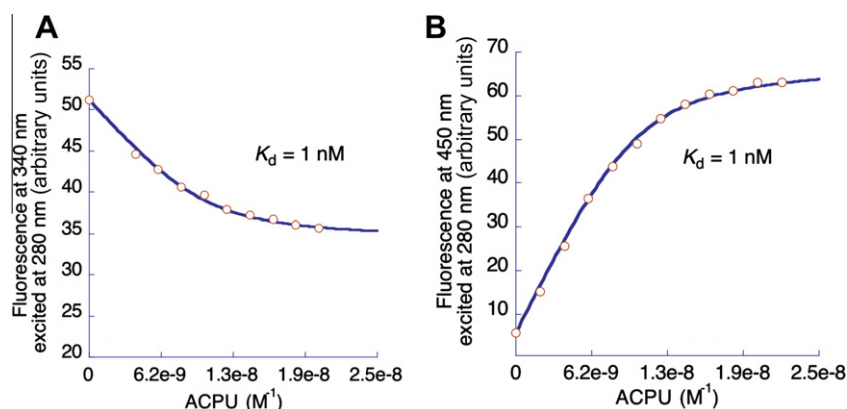


Fig. 2. Titration curve of hSEH with reporting ligand: ACPU monitored at 340 nm (A) and at 450 nm (B). Both are excited at 280 nm.

the relative occupancy of sEH by ACPU through its FRET signal at 450 nm as a function of the concentration of inhibitor. Here, the FRET signal at 450 nm was chosen because the emission at 330 nm from the sEH could result from interference not only by inhibitors that have aromatic pharmacophores but also by the changes of protein environment when inhibitors bind [16,35]. In addition, the FRET signal at 450 nm shows more significant change than the FRET signal at 330 nm (Fig. S5), which could help to improve the signal-to-noise ratio of the assay.

To determine the optimal temperature for the displacement assay, we investigated the rate of ACPU displacement by the sEH inhibitor, *t*-TUCB (**16**), at different temperatures. As expected, the rate for ACPU displacement by sEH inhibitors increases as a function of the temperature (Fig. S6). The time needed for reaching equilibrium on the addition of inhibitor decreased from 118 min at 25 °C to 75 min at 37 °C. Although increasing the temperature can shorten the time of reaching equilibrium by 15 min, the half-life of hSEH at 37 °C is 1.3 h, whereas at 30 °C it is 8.1 h [25]. Therefore, we decided to conduct the assay at 30 °C, and the incubation time for each titration was 90 min. (Only 5% of the fluorescence of the reporter-bound hSEH was diminished per hour [data not shown], indicating that the enzyme is stable throughout the displacement experiment [25].)

Through titration of the ACPU–hSEH complex with the sEH inhibitor, a decrease of fluorescence at 450 nm when excited at 280 nm was observed, indicating that the ACPU was displaced by the inhibitor (APAU, **2**) (Fig. 3). By plotting the relative fluorescence against the concentration of inhibitor, we obtain a displacement curve that can be used to calculate K_i of the inhibitors based on the K_d of ACPU by fitting the curve to the Wang-derived equation Eq. (5) [29].

The classic approach for K_i calculation is based on the Scatchard plot. This approach, which is used by most of the curve fitting

programs, assumes that less than 10% of added ligand is bound [40–42]. However, some of the sEH inhibitors we tested are very potent, with IC_{50} values below 1 nM. Therefore, these inhibitors would violate the assumptions associated with this classical approach. Wong reported a general equation Eq. (5) based on the three equilibrium states among inhibitor, ACPU, and targeted enzyme Eq. (4) to calculate the inhibition constant (K_i) of the inhibitor for competitive displacement assay. This approach provides a general equation to calculate the inhibition constant (K_i) from displacement assay without any assumptions [29]. The calculated K_i values of several compounds are shown in Table 1. In general, the K_i values determined with ACPU are lower than those obtained previously using *trans*-diphenyl-propene oxide (*t*-DPPO) in a catalytic assay. Besides being labor-intensive and expensive, this previously used assay could overestimate K_i values because a significant amount of the inhibitor was bound to the enzyme, which violates the assumption of the equation for K_i calculation [43].

To increase the throughput for displacement assay, it also was formatted for a 96-well plate. However, to obtain a fluorescent signal at 450 nm at least 5-fold above the background, 100 nM pure hSEH was needed (data not shown). The K_i values obtained from the 96-well plate assay correlated well with those determined by titration in a cuvette (Table 1). However, very potent compounds ($K_i < 1$ nM) need their inhibitory constant to be determined by titration in a cuvette because the nonlinear regression analysis can accurately calculate the K_i within two orders of magnitude of enzyme concentration [41].

Comparison of potency of sEH inhibitors using different assays

Several assays have been developed to measure the potency of sEH inhibitors since the first assay was reported; however, most of

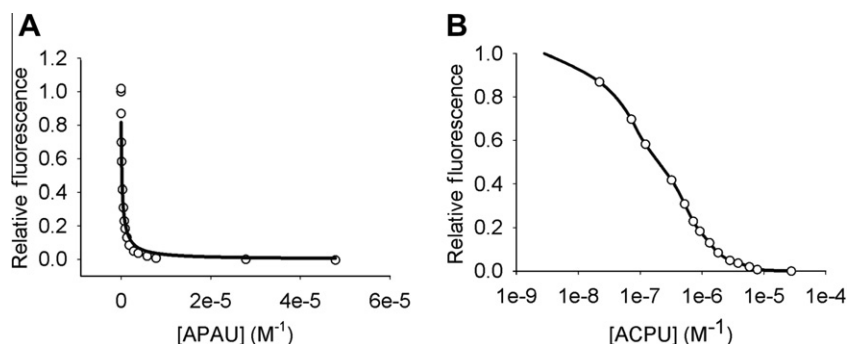


Fig. 3. (A) Displacement curve of hSEH–ACPU complex with sEH inhibitor APAU. The curve was fitted to a cubic equation derived from a three-state equilibrium. (B) Displacement curve of hSEH–ACPU complex with sEH APAU shown in log scale.

Table 1
Determination of sEH inhibitor potency for hsEH with different activity assays and K_i with the FRET-based displacement assay.

Inhibitor number (and name)	Reporter:	ACPU		<i>t</i> -DPPPO ^a		CMNPC ^b	EET ^c
	Structure	K_i^d (nM)		K_i^e (nM)	IC ₅₀ (nM)	IC ₅₀ (nM)	
	[E] ^f (nM):	10	100	2.5	2.5	2.5	2.5
1 (AUDA)		0.23 ± 0.07	0.11 ± 0.03	6.8 ± 0.2	14.8	6.2	143
2^f (APAU)		25.3	21.7 ± 3.10	125 ± 15	571	14	3913
3 (APBU)		2.62	3.02 ± 0.43	nd	10	3.8	272
4 (<i>t</i> -AUCB)		2.73 ± 1.50	1.93 ± 0.09	1.5 ± 0.2	3.7	2.0	251
5 (<i>t</i> -TUcol)		11.3	8.60 ± 0.57	nd	131	6.8	2913
6 (<i>t</i> -AUCM)		3.07	2.75 ± 0.72	nd	43	2.4	601
7 (<i>t</i> -TUCone)		25.2	nd	nd	667	21	3823
8 (TmPAU)		14.8	nd	nd	511	34	nd
9 (TPCU)		0.67	nd	nd	20	1.8	nd
10 (TmPPU)		Nd	2.96 ± 0.60	nd	48	9.3	398
11 (TmsBPU)		0.38 ± 0.04	0.41 ± 0.05	nd	9.5	2.5	226
12 (TmUPS)		Nd	7.16 ± 0.42	nd	79	13	1402
13 (TmUPSB)		Nd	0.98 ± 0.19	nd	15	3.1	417
14 (<i>t</i> -TUCB)		0.19	0.77 ± 0.11	9 ± 1	5.2	1.2	313
15 (TPPU)		0.57	0.73 ± 0.2	27 ± 2	34	nd	nd

Note: nd, not determined.

^a IC₅₀ was determined by the radiotracer assay using 50 μM *t*-DPPPO as a radiometric substrate with 2.5 nM purified recombinant hsEH at 30 °C for 10 min. The result is the average of duplicates.

^b IC₅₀ was determined by the fluorescence assay using 5 μM CMNPC as a fluorescent substrate with 2.5 nM purified recombinant hsEH at 30 °C for 10 min. The result is the average of triplicates.

^c IC₅₀ was determined by LC–MS/MS assay using 50 μM 14,15-EET as a substrate with 2.5 nM purified recombinant hsEH at 30 °C for 8 min. The result is the average of triplicates.

^d K_i was determined by FRET-based displacement assay using 1 equivalent of ACPU as a fluorescent reporter with 10 nM purified recombinant hsEH in cuvette-based assay and 100 nM purified recombinant enzyme in 96-well plate assay at 30 °C.

^e K_i was determined previously by catalytic-based assay using [³H] *t*-DPPO as substrate at 30 °C. Data are from the literature [42].

^f This inhibitor was used in human clinical trials and also is referred to as UC1153 or AR9281.

these are substrate based [5,11,21,44,45]. These substrate-based assays are attractive for mechanistic studies and allow one to prioritize the inhibitors with IC₅₀ values ranging from 0.4 to 100,000 nM. However, newer compounds have reached the limit of our fluorescent catalytic assay (IC₅₀ < 0.4 nM). Although other substrate-based assays, such as those using [³H] *t*-DPPO [14] (radiometric based) and 14,15-EET (LC–MS/MS assay) as a substrate, are able to distinguish among these potent compounds when [S] > [K_m], they are expensive and labor-intensive. The displacement assay is in simple equilibria among the inhibitor, ACPU, and sEH without the complication of the substrate catalysis in substrate-based assays. In addition, the displacement assay allows one to directly obtain the real affinity between inhibitors and enzyme and to measure the compounds with K_i down to 0.01 nM, which current substrate-based assays are unable to do.

To compare the displacement assay with different substrate-based assays, we tested the same series of compounds in the displacement assay against different substrate-based assays (Table 1). The IC₅₀ values we obtained from different substrate-based assays show some discrepancies, and this observation is consistent with the study of Tsai and coworkers [46]. The plot of K_i obtained from the displacement assay against IC₅₀ values from different assays shows that most of outlying points on the correction plot of IC₅₀ values are compounds with IC₅₀ values less than 5 nM with the fluorescent cyano(6-methoxy-naphthalen-2-yl)methyl *trans*-[(3-phenyloxyran-2-yl)methyl] carbonate (CMNPC) assay (Fig. S7). This suggests that many newly developed inhibitors have reached the limit of the fluorescent substrate assay to distinguish among them. Based on the Cheng–Prusoff equation, increasing substrate concentrations can increase the experimental IC₅₀ values of inhibitors. Because the radiometric assay and the LC–MS/MS assay use approximately 10 times higher concentrations of substrate than the K_m value of the respective substrate (Table S2), these assays can distinguish among very potent compounds better than the fluorescent CMNPC assay. Based on the Spearman's rank correlation coefficient analysis between the displacement assay and the other substrate-based assays (Table 2), the FRET displacement assay reported here correlated well with *t*-DPPO and 14,15-EET substrate-based assays and less well with the CMNPC fluorescent substrate assay. Thus, the CMNPC fluorescent substrate assay is a good way to rank compounds quickly, but reliability decreases as IC₅₀ values approach 5 nM, whereas the displacement assay provides a new way to distinguish among very potent sEH inhibitors.

Tsai and coworkers hypothesized that the discrepancy between fluorescent assay and radiometric assay was due in part to structural differences among inhibitors [46]. Here, compounds with different linkers, cyclohexyl-ether and piperidinyl, and substitutes on linkers with different size have been tested (Fig. S8). The results suggest that compounds with the largest discrepancy of IC₅₀ values in different assays are largely, but not totally, due to the fact that they reached the limit of the fluorescent CMNPC assay but not

the limit of the *t*-DPPO assay (Table 1, inhibitors 2, 5–8, 10, 12, and 15), whereas compounds with large substituents on the linker (Table 1, inhibitors 3, 4, 11, 13, and 14) are very potent and are close to the limit of both assays.

Development of FRET assay to measure relative *k*_{off} of sEH inhibitors

In addition to the K_i, which reflects the strength of drug–target interaction, the drug–target residence time of slow tight binding inhibitors has become another vital parameter for choosing leads among compounds for optimization in medicinal chemistry and testing in vivo [22,47]. Because the drug is effective only when the inhibitor is bound to the target protein or enzyme, determining the residence time, which describes the period of time when the drug is bound to enzyme, is important. Residence time should be an improved metric for predicting the in vivo potency because in vivo models are an open system compared with in vitro enzyme assays in which the K_i is measured in a closed system. In addition, K_i is the ratio of *k*_{on} to *k*_{off}. Because *k*_{on} of very potent compounds is limited by the diffusion of the molecules and *k*_{off} is solely the dissociation of the inhibitor from the enzyme, which is usually slow for potent inhibitors, a method to measure *k*_{off} is invaluable.

Here, inspired by the application note of Invitrogen's LanthaScreen Eu kinase binding assay kit, the FRET assay described above was further developed to measure the relative *k*_{off} of sEH inhibitors. When the enzyme–inhibitor complexes are diluted, the inhibitor is dissociated from the enzyme and the free enzyme is trapped by a large excess of ACPU quickly and FRET occurs (see Scheme S1 in Supplementary material). By monitoring the FRET signal (excitation at 280 nm and emission at 450 nm) over time, we can determine *k*_{off} of the sEH inhibitor through fitting to a first-order exponential growth curve (Fig. 4). The fastest inhibitor takes approximately 5000 s (~80 min) to be completely dissociated from the enzyme. Therefore, only the data obtained during the first 5000 s was used for determining *k*_{off} (Table 3). In addition, a relative short time of analysis reduces the risk of secondary reactions, such as the rebinding of inhibitor to sEH and the degradation of enzyme–inhibitor complex, that could affect the analysis.

To determine whether 40 times dilution of the enzyme–inhibitor complex with a 100-fold excess of ACPU can bind the free enzyme quick enough to prevent the inhibitor from displacing

Table 2
Spearman's rank correlation coefficient across different sEH catalytic assays.

Reporter	CMNPC	[³ H] <i>t</i> -DPPO	14,15-EET
ACPU	.75	.88	.92
CMNPC	–	.86	.65
[³ H] <i>t</i> -DPPO	–	–	.90

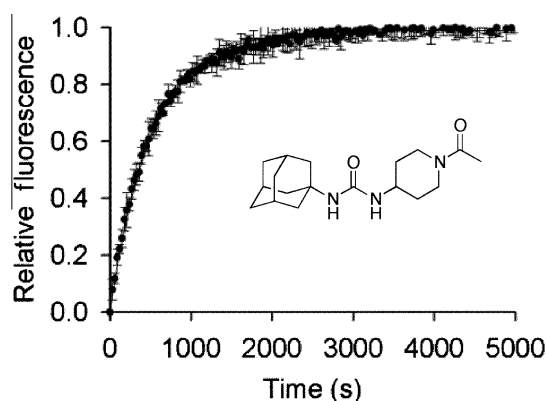


Fig. 4. *k*_{off} determination of APAU (UC1153) using the FRET system described.

the enzyme–ACPU during the first 5000 s, we conducted an experiment by varying the amount of ACPU (50- and 200-fold excesses) to dilute enzyme–inhibitor complex (Table 4). If the condition we used is not high enough to prevent the inhibitor from displacing the sEH–ACPU complex, the observed k_{off} will be greatly affected by dilution of the complex with different amounts of ACPU. Although we observed a slight increase of the k_{off} value when we increased the amount of ACPU used for dilution of the enzyme–inhibitor complex from 50-fold to 100-fold excess of ACPU, we did not observe much change of the k_{off} value when we further increased the amount of ACPU from 100-fold excess to 200-fold excess. The results indicated that 100-fold excess of ACPU is enough to prevent the displacement of ACPU from enzyme–ACPU complex by inhibitor.

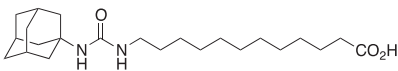
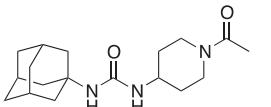
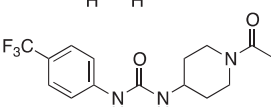
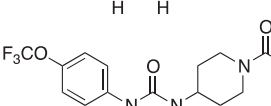
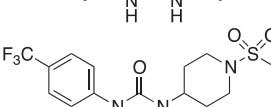
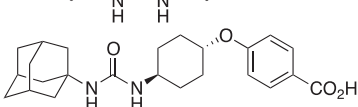
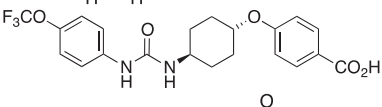
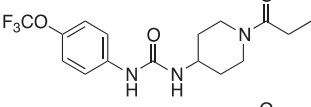
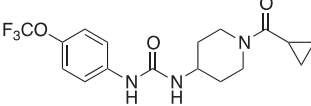
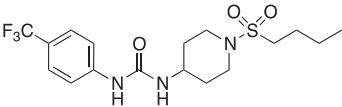
The observed k_{off} for hsEH showed that it is well correlated with the size of the inhibitor but not the K_i of the inhibitor. As the size of the inhibitor increased, the observed k_{off} decreased (slower). We found that the adamantyl group on the left side of the urea gives the slowest k_{off} , followed by 4-trifluoromethoxyphenyl and trifluoromethyl (Table 3, from second to fourth entries and sixth to sev-

enth entries). In addition, we found that sulfonamide on the piperidine linker leads to release from the hsEH much faster than the amide (Table 3, second and fifth entries).

Determination of K_i and k_{off} of sEH inhibitors from other species sEH with ACPU

Based on the sequence analysis, rodent and murine sEH showed greater than 76% sequence identity to hsEH. Therefore, ACPU should be able to measure K_i of sEH inhibitors on sEH from other species. Although we were able to determine K_d of the reporter on both murine sEH ($K_d = 0.1$ nM) and rat sEH ($K_d = 0.17$ nM), we were unable to completely displace the bound ACPU from the rat sEH even with an excess of very potent sEH inhibitor (*t*-TUCB) within a reasonable period of time (3 h). Therefore, we could obtain only the K_i values of sEH inhibitors against murine sEH (compound **2**, 1.86 nM; compound **14**, 6.22 nM; and compound **13**, 1.08 nM). Based on these results, mouse sEH (msEH) binds sEH inhibitors with an adamantyl substituent much tighter than hsEH (compound **2**, hsEH = 21.7 nM, msEH = 1.86 nM).

Table 3
 k_{off} measurements of different sEH inhibitors from sEH from different species.

Inhibitor number (and name)	sEH inhibitor structure	Human sEH	Mouse sEH	Rat sEH
		[observed k_{off} (10^{-3} s $^{-1}$)/ $T_{1/2}$ (min)]		
1 (AUDA)		0.9/13	nd	nd
2 (APAU)		1.9/6	0.37/31	0.29/40
8 (TmPAU)		3.0/4	1.7/7	0.93/12
16 (TPAU)		2.6/4	1.9/6	0.97/12
12 (TmUPS)		2.3/5	1.2/10	0.5/23
4 (<i>t</i> -AUCB)		0.38/30	0.44/26	0.23/50
14 (<i>t</i> -TUCB)		0.72/16	0.49/24	0.98/12
15 (TPPU)		1.1/11	0.58/20	0.91/13
9 (TPCU)		0.66/18	0.49/24	nd
13 (TmUPS _B)		1.0/12	0.42/28	0.36/32

Note: The preincubated enzyme–inhibitor (8 μ M) was diluted 40 times with 100 equivalents of ACPU (20 μ M, 100 mM sodium phosphate, pH 7.4) at 25 °C. nd, not determined.

Table 4 k_{off} measured from hsEH with different equivalents of ACPU.

Inhibitor number (and name)	50-Equivalent excess of ACPU [observed k_{off} (10^{-3} s^{-1})]	100-Equivalent excess of ACPU	200-Equivalent excess of ACPU
4 (<i>t</i> -AUCB)	0.30	0.38	0.40
11 (TmsBPU)	0.54	0.58	0.54
2 (APAU)	1.7	1.9	1.7
8 (TmPAU)	2.2	3.0	2.7

Note: The preincubated enzyme–inhibitor (8 μM) was diluted 40 times with different equivalents of ACPU in PB buffer (100 mM sodium phosphate, pH 7.4) at 25 °C.

In addition, using ACPU, k_{off} values for sEH inhibitors against both murine and rat sEH were obtained (Table 3). Compounds containing adamantyl group had a much slower k_{off} for mouse sEH and rat sEH as compared with human sEH. (Table 3, second and fifth entries). These results suggest that there may be difficulty in translation of the efficacy of sEH inhibitors obtained from in vivo rat and mouse model to human because the human enzyme has very different K_i and k_{off} values as compared with those of rat and mouse.

Conclusion

Here, we have reported a new fluorescent reporter, ACPU, that can be used to determine the accurate K_i of sEH inhibitors by competitive displacement assay down to sub-nanomolar or picomolar levels using a 96-well plate-based assay or a cuvette-based assay, respectively. In addition, ACPU was further used for k_{off} determination of sEH inhibitors. k_{off} has become an important parameter to predict in vivo potency. This assay is the first reported fluorescence-based assay to measure the relative k_{off} for sEH inhibitors and has been adapted to a 96-well plate format that can provide an alternative way to screen and measure the potency of sEH inhibitors.

During the assay development, several parameters were optimized for effective K_i or k_{off} measurement for potent inhibitors. K_d of the reporting ligand must be low, and the quantum yield for the reporting ligand must be high, so that a low concentration of the targeted enzyme can be used. In addition, k_{on} of the reporting ligand must be fast enough to yield a practical k_{off} measurement. However, the k_{off} of the reporting ligand should not be too slow; otherwise, it would be impractical for K_i determination.

Whereas the previous substrate-based assays either are unable to measure the K_i for sEH inhibitors or are labor-intensive, the current competitive displacement assay is easier and cheaper to use. In addition, we showed that the current assay could be adapted to a 96-well plate format that can facilitate the screening of newly synthesized sEH inhibitors, which usually are too potent for CMNPC fluorescent assay to distinguish among them.

It is suspected, albeit not proven, that fatty acid epoxides from ω -3 and ω -6 series are endogenous substrates [1,8]. These substrates will compete with sEH inhibitors in vivo as a function of concentration and properties of inhibitor, but they also will compete as a function of concentration and affinity of endogenous substrates. A good correlation between K_i values obtained from FRET-based displacement assay and IC_{50} values determined by LC–MS/MS using 14,15-EET as a substrate suggested that the FRET displacement assay could predict the in vivo potency for the inhibitors.

Based on these reasons, the FRET-based displacement assay reported here provides an alternative and possibly improved way to predict the in vivo potency of sEH inhibitors.

Acknowledgments

This work was partially funded by National Institute of Environmental Health Sciences (NIEHS) grant ES002710, NIEHS Superfund Research Program grant P42 ES04699, and National Institutes of Health (NIH) Counter Act Program U54 NS079202-01. B.D.H. is a George and Judy Marcus Senior Fellow of the American Asthma Foundation.

Appendix A. Supplementary data

Supplementary data associated with this article can be found, in the online version, at <http://dx.doi.org/10.1016/j.ab.2012.11.015>.

References

- [1] J.W. Newman, C. Morisseau, B.D. Hammock, Epoxide hydrolases: their roles and interactions with lipid metabolism, *Prog. Lipid Res.* 44 (2005) 1–51.
- [2] D. Ai, W. Pang, N. Li, M. Xu, P.D. Jones, J. Yang, Y. Zhang, N. Chiamvimonvat, J.Y.J. Shyy, B.D. Hammock, Y. Zhu, Soluble epoxide hydrolase plays an essential role in angiotensin II-induced cardiac hypertrophy, *Proc. Natl. Acad. Sci. U.S.A.* 106 (2009) 564–569.
- [3] B.B. Davis, D.A. Thompson, L.L. Howard, C. Morisseau, B.D. Hammock, R.H. Weiss, Inhibitors of soluble epoxide hydrolase attenuate vascular smooth muscle cell proliferation, *Proc. Natl. Acad. Sci. U.S.A.* 99 (2002) 2222–2227.
- [4] C. Morin, M. Sirois, V. Echave, M.M. Gomes, E. Rousseau, EET displays anti-inflammatory effects in TNF- α -stimulated human bronchi, *Am. J. Respir. Cell Mol. Biol.* 38 (2008) 192–201.
- [5] T.E. Rose, C. Morisseau, J.-Y. Liu, B. Inceoglu, P.D. Jones, J.R. Sanborn, B.D. Hammock, 1-Aryl-3-(1-acylpiperidin-4-yl)urea inhibitors of human and murine soluble epoxide hydrolase: structure–activity relationships, pharmacokinetics, and reduction of inflammatory pain, *J. Med. Chem.* 53 (2010) 7067–7075.
- [6] K.R. Schmelzer, L. Kubala, J.W. Newman, L.H. Kim, J.P. Eiserich, B.D. Hammock, Soluble epoxide hydrolase is a therapeutic target for acute inflammation, *Proc. Natl. Acad. Sci. U.S.A.* 102 (2005) 9772–9777.
- [7] A.N. Simpkins, R.D. Rudic, D.A. Schreihofner, S. Roy, M. Manhiani, H.-J. Tsai, B.D. Hammock, J.D. Imig, Soluble epoxide inhibition is protective against cerebral ischemia via vascular and neural protection, *Am. J. Pathol.* 174 (2009) 2086–2095.
- [8] B. Inceoglu, K. Wagner, N.H. Schebb, C. Morisseau, S.L. Jinks, A. Ulu, C. Hegedus, T. Rose, R. Brosnan, B.D. Hammock, Analgesia mediated by soluble epoxide hydrolase inhibitors is dependent on cAMP, *Proc. Natl. Acad. Sci. U.S.A.* 108 (2011) 5093–5097.
- [9] Y.-X. J. Wang, A. Ulu, L.-N. Zhang, B. Hammock, Soluble epoxide hydrolase in atherosclerosis, *Curr. Atheroscler. Rep.* 12 (2010) 174–183.
- [10] H.C. Shen, B.D. Hammock, Discovery of inhibitors of soluble epoxide hydrolase: a target with multiple potential therapeutic indications, *J. Med. Chem.* 55 (2012) 1789–1808.
- [11] S.S. Gill, S.I. Wie, T.M. Guenther, F. Oesch, B.D. Hammock, Rapid and sensitive enzyme-linked immunosorbent assay for the microsomal epoxide hydrolase, *Carcinogenesis* 3 (1982) 1307–1310.
- [12] R.N. Wixtrom, B.D. Hammock, Continuous spectrophotometric assays for cytosolic epoxide hydrolase, *Anal. Biochem.* 174 (1988) 291–299.
- [13] A.B. Eldrup, F. Soleymanzadeh, S.J. Taylor, I. Muegge, N.A. Farrow, D. Joseph, K. McKellop, C.C. Man, A. Kukulka, S. De Lombaert, Structure-based optimization of arylamides as inhibitors of soluble epoxide hydrolase, *J. Med. Chem.* 52 (2009) 5880–5895.
- [14] B. Borhan, T. Mebrahtu, S. Nazarian, M.J. Kurth, B.D. Hammock, Improved radiolabeled substrates for soluble epoxide hydrolase, *Anal. Biochem.* 231 (1995) 188–200.
- [15] P.D. Jones, N.M. Wolf, C. Morisseau, P. Whetstone, B. Hock, B.D. Hammock, Fluorescent substrates for soluble epoxide hydrolase and application to inhibition studies, *Anal. Biochem.* 343 (2005) 66–75.
- [16] E.G. Matveeva, C. Morisseau, M.H. Goodrow, C. Mullin, B.D. Hammock, Tryptophan fluorescence quenching by enzyme inhibitors as a tool for enzyme active site structure investigation: epoxide hydrolase, *Curr. Pharm. Biotechnol.* 10 (2009) 589–599.
- [17] N.H. Schebb, M. Huby, C. Morisseau, S.H. Hwang, B.D. Hammock, Development of an online SPE–LC–MS-based assay using endogenous substrate for investigation of soluble epoxide hydrolase (sEH) inhibitors, *Anal. Bioanal. Chem.* 400 (2011) 1359–1366.
- [18] N.M. Wolf, C. Morisseau, P.D. Jones, B. Hock, B.D. Hammock, Development of a high-throughput screen for soluble epoxide hydrolase inhibition, *Anal. Biochem.* 355 (2006) 71–80.
- [19] M. Arand, A. Cronin, M. Adamska, F. Oesch, Epoxide hydrolases: structure, function, mechanism, and assay, in: S. Helmut, P. Lester (Eds.), *Methods in Enzymology*, Academic Press, San Diego, 2005, pp. 569–588.
- [20] R.N. Wixtrom, B.D. Hammock, Membrane-bound and soluble-fraction epoxide hydrolases: methodological aspects, *Biochem. Pharmacol. Toxicol.* 1 (1985) 1–93.
- [21] S.H. Hwang, H.-J. Tsai, J.-Y. Liu, C. Morisseau, B.D. Hammock, Orally bioavailable potent soluble epoxide hydrolase inhibitors, *J. Med. Chem.* 50 (2007) 3825–3840.

- [22] L.J. Marnett, The COXIB experience: a look in the rearview mirror, *Annu. Rev. Pharmacol. Toxicol.* 49 (2009) 265–290.
- [23] P.D. Jones, H.-J. Tsai, Z.N. Do, C. Morisseau, B.D. Hammock, Synthesis and SAR of conformationally restricted inhibitors of soluble epoxide hydrolase, *Bioorg. Med. Chem. Lett.* 16 (2006) 5212–5216.
- [24] B.D. Hammock, S.H. Hwang, A.T. Weckler, C. Morisseau, Sorafenib derivatives as sEH inhibitors, WIPO application WO/2012/112570 (2012).
- [25] C. Morisseau, J.K. Beetham, F. Pinot, S. Debernard, J.W. Newman, B.D. Hammock, Cress and potato soluble epoxide hydrolases: purification, biochemical characterization, and comparison to mammalian enzymes, *Arch. Biochem. Biophys.* 378 (2000) 321–332.
- [26] K.S.S. Lee, T. Berbasova, C. Vasileiou, X. Jia, W. Wang, Y. Choi, F. Nossoni, J.H. Geiger, B. Borhan, Probing wavelength regulation with an engineered rhodopsin mimic and a C15-retinal analogue, *ChemPlusChem* 77 (2012) 273–276.
- [27] C. Vasileiou, S. Vaezeslami, R.M. Crist, M. Rabago-Smith, J.H. Geiger, B. Borhan, Protein design: reengineering cellular retinoic acid binding protein II into a rhodopsin protein mimic, *J. Am. Chem. Soc.* 129 (2007) 6140–6148.
- [28] L. Wang, Y. Li, H. Yan, Structure–function relationships of cellular retinoic acid-binding proteins, *J. Biol. Chem.* 272 (1997) 1541–1547.
- [29] Z.X. Wang, An exact mathematical expression for describing competitive binding of two different ligands to a protein molecule, *FEBS Lett.* 360 (1995) 111–114.
- [30] M.H.A. Roehrl, S.H. Kang, J. Aramburu, G. Wagner, A. Rao, P.G. Hogan, Selective inhibition of calcineurin–NFAT signaling by blocking protein–protein interaction with small organic molecules, *Proc. Natl. Acad. Sci. U.S.A.* 101 (2004) 7554–7559.
- [31] A. Cronin, S. Mowbray, H. Durk, S. Homburg, I. Fleming, B. Fisslthaler, F. Oesch, M. Arand, The N-terminal domain of mammalian soluble epoxide hydrolase is a phosphatase, *Proc. Natl. Acad. Sci. U.S.A.* 100 (2003) 1552–1557.
- [32] G.A. Gomez, C. Morisseau, B.D. Hammock, D.W. Christianson, Structure of human epoxide hydrolase reveals mechanistic inferences on bifunctional catalysis in epoxide and phosphate ester hydrolysis, *Biochemistry* 43 (2004) 4716–4723.
- [33] G.A. Gomez, C. Morisseau, B.D. Hammock, D.W. Christianson, Human soluble epoxide hydrolase: structural basis of inhibition by 4-(3-cyclohexylureido)-carboxylic acids, *Protein Sci.* 15 (2006) 58–64.
- [34] A.W. Norris, L. Cheng, V. Giguere, M. Rosenberger, E. Li, Measurement of subnanomolar retinoic acid-binding affinities for cellular retinoic acid-binding proteins by fluorometric titration, *Biochim. Biophys. Acta* 1209 (1994) 10–18.
- [35] J.T. Vivian, P.R. Callis, Mechanisms of tryptophan fluorescence shifts in proteins, *Biophys. J.* 80 (2001) 2093–2109.
- [36] L.D. Lavis, R.T. Raines, Bright ideas for chemical biology, *ACS Chem. Biol.* 3 (2008) 142–155.
- [37] X.Y. Huang, Fluorescence polarization competition assay: the range of resolvable inhibitor potency is limited by the affinity of the fluorescent ligand, *J. Biomol. Screen.* 8 (2003) 34–38.
- [38] B. Birdsall, R.W. King, M.R. Wheeler, C.A. Lewis, S.R. Goode, R.B. Dunlap, G.C.K. Roberts, Correction for light-absorption in fluorescence studies of protein–ligand interactions, *Anal. Biochem.* 132 (1983) 353–361.
- [39] X.Y. Huang, Equilibrium competition binding assay: inhibition mechanism from a single dose response, *J. Theor. Biol.* 225 (2003) 369–376.
- [40] R.A. Copeland, Evaluation of Enzyme Inhibitors in Drug Discovery: A Guide for Medicinal Chemists and Pharmacologists (Methods of Biochemical Analysis), John Wiley, Hoboken, NJ, 2005.
- [41] R.A. Copeland, Enzymes: A Practical Introduction to Structure, Mechanism, and Data Analysis, John Wiley, New York, 2000.
- [42] H.J. Motulsky, A. Christopoulos, Fitting Models to Biological Data Using Linear and Nonlinear Regression: A Practical Guide to Curve Fitting, GraphPad Software, San Diego, 2003.
- [43] J.-Y. Liu, S.-H. Park, C. Morisseau, S.H. Hwang, B.D. Hammock, R.H. Weiss, Sorafenib has soluble epoxide hydrolase inhibitory activity, which contributes to its effect profile in vivo, *Mol. Cancer Ther.* 8 (2009) 2193–2203.
- [44] L.S. Hasegawa, B.D. Hammock, Spectrophotometric assay for mammalian cytosolic epoxide hydrolase using *trans*-stilbene oxide as the substrate, *Biochem. Pharmacol.* 31 (1982) 1979–1984.
- [45] C.A. Mullin, B.D. Hammock, A rapid radiometric assay for mammalian cytosolic epoxide hydrolase, *Anal. Biochem.* 106 (1980) 476–485.
- [46] H.-J. Tsai, S.H. Hwang, C. Morisseau, J. Yang, P.D. Jones, T. Kasagami, I.-H. Kim, B.D. Hammock, Pharmacokinetic screening of soluble epoxide hydrolase inhibitors in dogs, *Eur. J. Pharm. Sci.* 40 (2010) 222–238.
- [47] M.M. Hann, G.M. Keserue, Finding the sweet spot: the role of nature and nurture in medicinal chemistry, *Nat. Rev. Drug Discov.* 11 (2012) 355–365.